Research on Electromagnetic Damage Effects in Navigation Receiver by PCI Testing

Meng Zhang [1], Zhong Fang [1], Yu Hao [1], Wei Du[1], Xuchao Pan[1], Junjie Jiao[1], Yong He[1,a,*]

[1] school of mechanical engineering, Nanjing University of Science and Technology, Jiangsu, 210094, China;

[a] yonghe1964@163.com

Abstract. The EMP couples with electronic devices via cables, inducing electromagnetic damage effects. This paper elucidates the operational principles of a navigation receiver and simplifies the study by focusing on the radio frequency front-end module. Many PCI tests were conducted on its signal input port, yielding the damage threshold of the navigation receiver. An analysis of the output waveforms of the modules that incurred damage was also performed. Through infrared research, it was discovered that the damaged LNA experiences a rapid temperature rise to around 73°C during operation with applied power. The electromagnetic damage effect in the LNA primarily stems from internal MOS transistor short circuits. The BPF protects the subsequent circuit stages but is also susceptible to damage.

Keywords: pulse current injection; UAV; EMP; navigation receiver; electromagnetic sensitivity.

1. Introduction

In the Russia-Ukraine conflict, the widespread utilization of UAV (Unmanned Aerial Vehicle) systems has demonstrated their crucial role in surveillance, command, strike capabilities, and information warfare [1]. Navigation receivers play a critical role by providing precise positioning information to these UAVs, enabling all-weather operations [2]. However, as highly integrated electronic devices, navigation receivers are vulnerable to the external electromagnetic environment. EMP (Electromagnetic Pulse) weapons generate electromagnetic pulses that can couple and propagate through cables, antennas, and apertures, ultimately leading to damage in the electronic circuits [3-5]. Consequently, the electromagnetic damage effects of navigation receivers under EMP exposure are a significant focal point in the research on UAV attack and defense strategies.

Numerous scholars have conducted extensive research on the electromagnetic damage issues concerning navigation receivers. Torreo et al. tested UAV under an electromagnetic field intensity of 10 V/m. The results indicated that, compared to other electronic devices, the GPS module was more susceptible to the effects of interference signals [6]. Fan Yuqing et al. experimentally demonstrated the feasibility of using radio frequency injection instead of radio frequency irradiation in continuous wave interference tests to validate BDS (Bei Dou Satellite System) receivers [7]. Huang Xin et al. conducted controlled wave irradiation experiments on navigation receivers, focusing on the electromagnetic pulse's coupling into data monitoring terminals through cables, causing power supply voltage disturbances and forcing system reboots [8]. Scholars have laid a particular foundation for the issue of navigation receiver electromagnetic damage. However, they did not extensively study the damage patterns of the navigation receiver, and systematic analysis of the receiver's sensitive components was also absent.

This study begins by analyzing the navigation receiver system and adopts the RF (radio frequency) front-end module of the navigation receiver as the subject of experimentation. The distribution pattern of its damage threshold is obtained through extensive PCI (Pulse Current Injection) tests on the RF front-end module. Concurrently, vulnerability analysis of sensitive components is conducted, providing a theoretical basis for protective measures of navigation receivers.

2. Analysis of the Navigation Receiver System

The navigation receiver system generally consists of three major functional modules: antenna, RF front-end processing, baseband digital signal processing (DSP), and CPU, as shown in Figure 1. The navigation receiver antenna captures satellite carrier signals transmitted via coaxial cables to the RF front-end processing module. The signals are filtered and amplified after passing through BPF (Band Pass Filter) and LNA (Low Noise Amplifier). Using a mixer, the signs are mixed with a local oscillator's sinusoidal wave, and intermediate frequency filters filter out high-frequency signals. Subsequently, they are down-converted to intermediate frequency (IF) signals and transformed into digital IF signals through analog-to-digital converters. The baseband signal processing module processes the digital intermediate frequency signals to capture and track the satellite-transmitted signals, obtaining measurements such as carrier phase and pseudo-range to enable precise positioning [9-11].

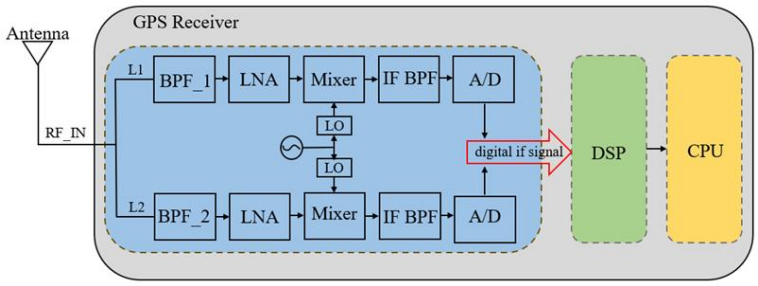

(a) Navigation Receiver System Diagram

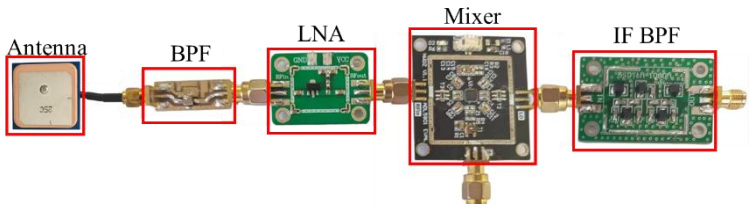

(b) the RF front-end module

Figure. 1 Navigation Receiver System

Cables are a significant pathway for coupling EMP effects [12-14]. Navigation receivers employ a signal cable to transmit satellite signals the antenna receives. The radio frequency front-end module, DSP, and CPU are typically integrated. Consequently, signal cables between these modules can be omitted, while signals for transmitting satellite signals unavoidably couple with EMP [15-17]. Positioned at the forefront of the navigation receiver, the RF front-end module represents the module most susceptible to electromagnetic damage effects [18]. For simplification, the RF front-end module was chosen as the focal point of the study. Focusing on the signal input port, a single wire was used as the EMP coupling cable to conduct PCI experiments.

3. PCI Testing of Navigation Receivers

3.1 PCI Test Design of Navigation Receivers

The PCI test refers to a method involving the injection of all currents in the EMP-conducted environment [19]. Conducting PCI tests on the RF front-end module enables an adequate emulation of its electromagnetic damage characteristics under HEMP irradiation. In this study, the EMPC2000 pulse source is employed, capable of generating a double-exponential pulse with a rise time of less than 20ns and a pulse width ranging from 500ns to 550ns [20]. The pulse amplitude can be adjusted between 20A and 2000A. The injected pulse waveform is depicted in Figure 2.

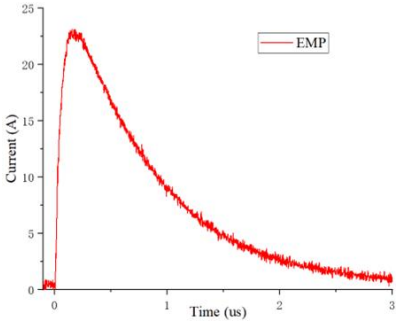

Figure. 2 Actual Injected EMP Waveform

Following the configuration shown in Figure 3, the injection system, radio frequency front-end module, and test system (Rogowski coil) were interconnected. Prior to commencing the experiment, the radio frequency front-end module was tested to ensure its proper functioning. With the module powered and functioning normally, pulsed current injections were applied to the module's signal input port. The peak value of the pulsed current I_0, was utilized as the variable in these experiments. The actual injected pulse was measured using the Rogowski coil, and the corresponding data were documented.

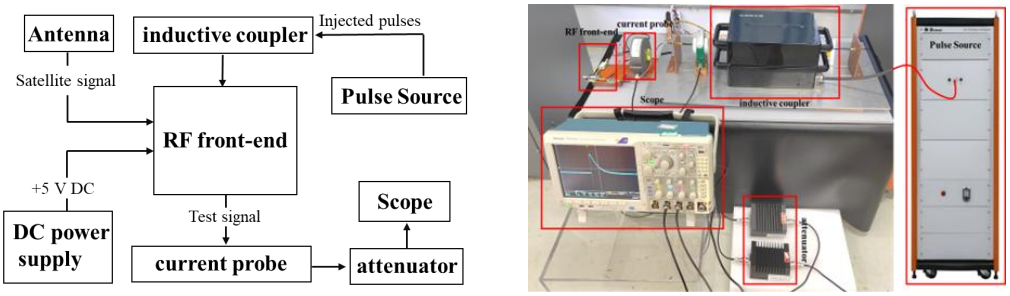

(a) Test system layout (b) Field test system

Figure. 3 PCI Test Layout

3.2 PCI Test Results

The damage was assessed by contrasting the module's output waveform with its waveform during regular operation. When the RF front-end module experiences electromagnetic vulnerability effects, it exhibits two states: reduction (represented by 'R') and damage (represented by 'D'). When no electromagnetic vulnerability effects are observed, it is recorded as 'N' The module damage threshold is presented in Table 1.

Table 1. RF Front-End Module Damage Threshold

NO.	I_0(/A)	BPF	LNA	Module	Repeat
1	20	N	N	N	1
2	30	N	N	N	1
3	40	N	N	N	1
4	50	N	N	N	1
5	60	R	N	R	1
6	60	N	N	N	2
7	70	R	D	R	2
8	70	R	N	R	1
9	80	D	D	D	3

As shown in Figure 4, the RF front-end module exhibits an electromagnetic damage effect characterized by a linear variation. Both the BPF and the LNA experience impairment, resulting in attenuation of the input signal. When the input signal is mixed with the local oscillator (LO) signal

during frequency conversion, the dominant influencing factor is the LO signal. Consequently, the output signal manifests as a sinusoidal waveform, with only the amplitude gradually diminishing. In the scenario where the IF BPF remains undamaged, it effectively filters out spurious signals generated during mixing, thereby maintaining the frequency integrity of the output signal.

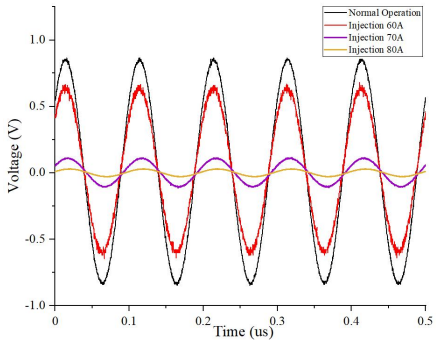

Figure. 4 Output Waveform of RF Front-End Module after Damage

Testing the modules that exhibited damage effects showed that the primary components affected were the BPF and LNA. At the same time, the subsequent mixer and intermediate frequency filters did not show damage effects. The output signal amplitude of the BPF gradually decreased, and when the injected pulse peak current reached 80A, complete failure occurred, with almost no signal output. As shown in Figure 5, after the damage to the LNA, the output signal frequency changed from around 1.5GHz to approximately 500KHz, and its amplification function was lost, resulting in signal attenuation instead. A comparative experiment was conducted with an intact LNA to validate the damage condition of the LNA further. In Figure 6, the undamaged LNA, when powered, exhibited a stable temperature increase up to 35°C. In contrast, the temperature of the LNA, following physical damage, rapidly rose to 73°C upon powering and continued to escalate. The experiment results suggest the possibility of extensive short-circuiting in the internal MOS transistors of the amplifier.

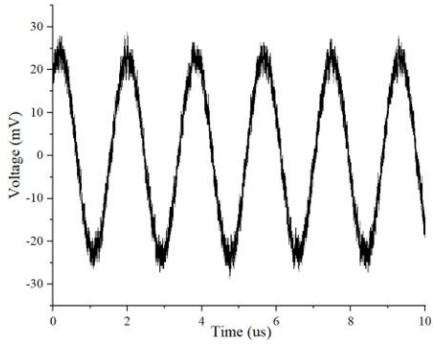

Figure. 5 Typical Output Waveform of Damaged LNA

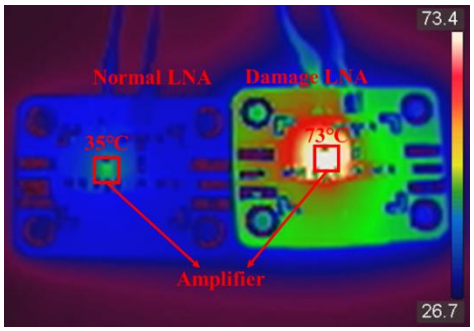

Figure. 6 Temperature of Damaged LNA

In the PCI test conducted on the RF front-end module without the BPF, the LNA exhibited damage effects even at an injected pulse peak current of only 20A, while the subsequent mixer and

IF BPF remained undamaged. The damaged LNA did not display rapid temperature rise upon powering it on, and the output signal experienced an attenuation of approximately 40 times, accompanied by interference signals, as shown in Figure 7. By comparing these results with the previous experiments, it is evident that the filters provide some protection to the subsequent amplifier when they are undamaged.

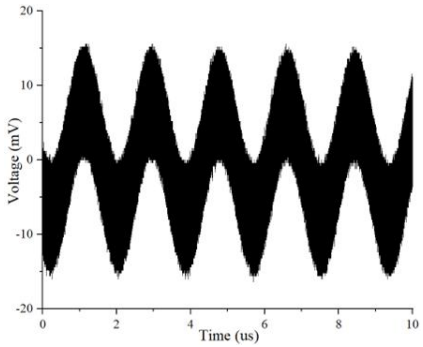

Figure. 7 Output Signal of Damaged LNA with 20A Injected Current

4. Summary

The RF front-end module of the receiver was selected as the research object to obtain the electromagnetic damage threshold of the navigation receiver. The PCI test was conducted by injecting pulses into the signal lines after the antenna. The results showed that the BPF and the LNA were prone to damage effects. Additionally, the BPF consistently exhibited damage effects earlier than the LNA. On the other hand, the damage to the LNA was mainly focused on internal short circuits within the transistor, resulting in the loss of amplification functionality.

The damage to both front-end components would lead to degradation or a complete failure for the entire receiver system. Although the BPF offered some protection to the subsequent parts, it was still susceptible to damage effects. The receiver can be effectively safeguarded by incorporating electromagnetic shielding circuits such as limiters and splitters in the RF front-end, enhancing its electromagnetic damage threshold.

References

[1] Yang Jihui, Zhu Chaolei, Xu Jia. Analysis of UAV deployment in the Russia-Ukraine conflict[J]. Tactical Missile Technology,2022(3):116-123.

[2] Gyagenda N, Hatilima J V, Roth H, et al. A review of GNSS-independent UAV navigation techniques[J]. Robotics and Autonomous Systems, 2022, 152: 104069.

[3] Meiling Z, Jinliang C, Zao Y, et al. Effect of aperture on shielding performance of metal cavity under excitation of high-intensity electromagnetic pulse[J]. High Power Laser and Particle Beams, 2021, 33(4): 043004-1-043004-10.

[4] Hu X, Qiu Y, Xu Q, et al. Transient response of microstrip patch antenna loaded on a vehicle platform illuminated by electromagnetic pulse[J]. Progress In Electromagnetics Research C, 2020, 104: 69-84.

[5] ZHANG Y, SHANG Y P. Review on the study of EMP-to-transmission line coupling problem[J]. Journal of Microwaves, 2020, 36(1): 103-110.

[6] Torrero L , Mollo P , Molino A ,et al. RF immunity testing of an Unmanned Aerial Vehicle platform under strong EM field conditions[C]//European Conference on Antennas & Propagation. IEEE, 2013.

[7] Fan Y , Cheng E , Wei M ,et al. Effects of CW Interference on the BDS Receiver and Analysis on the Coupling Path of Electromagnetic Energy[J]. IEEE Access, 2019, PP(99):1-1.

[8] Huang X, Chen Y Z, Wang Y M, et al. Research on irradiation effect of nuclear electromagnetic pulse on navigation receiving system [J]. Journal of Sichuan Ordnance, 2022(002):043.

[9] Xie Gang. GPS principle and receiver design [M]. Electronic Industry Press,2009.

[10] Ivanov S. PRINCIPLES OF GNSS: PRINCIPLES OF GNSS[J]. Journal scientific and applied research, 2021, 20(1): 27-32.

[11] Li X, Wang B, Li X, et al. Principle and performance of multi-frequency and multi-GNSS PPP-RTK[J]. Satellite Navigation, 2022, 3(1): 7.

[12] Liao C, Zhang Y, Shang YP, Huan R. Review on the study of EMP to transmission line coupling problem. J Microw 2020;36(1):103e10.

[13] Gassab O, Yin WY. Characterization of electromagnetic wave coupling with a twisted bundle of twisted wire pairs (TBTWPs) above a ground plane. IEEE Trans Electromagn C 2019;61(1):241e60.

[14] Rashid R, Gilani S A A. Electromagnetic Pulse (EMP): A study of general trends, simulation analysis of E1 HEMP coupling and protection strategies[C]//2021 International Conference on Cyber Warfare and Security (ICCWS). IEEE, 2021: 106-111.

[15] Daojie Y, Kai H, Baisen G, et al. Failure process and mechanism of irradiation interference in unmanned aerial vehicle positioning system[J]. High Power Laser and Particle Beams, 2023, 35(2): 023002-1-023002-9.

[16] Gao C, Xue Z, Li W, et al. The influence of electromagnetic interference of HPM on UAV[C]//2021 International Conference on Microwave and Millimeter Wave Technology (ICMMT). IEEE, 2021: 1-3.

[17] Tongcheng Z, Daojie Y, Dongfang Z, et al. Ultra-wide spectrum electromagnetic pulse effect and experimental analysis of UAV GPS receiver[J]. High Power Laser and Particle Beams, 2019, 31(2): 023001-1-023001-5.

[18] Chang L, Hanyu L, Xianfeng B, et al. Electromagnetic pulse effect simulation and rating of RF front-end of super-heterodyne receiver[J]. High Power Laser and Particle Beams, 2021, 33(12): 123016-1-123016-6.

[19] Zhou Y, Xie Y Z, Zhang D Z, et al. Modeling and performance evaluation of inductive couplers for pulsed current injection[J]. IEEE Transactions on Electromagnetic Compatibility, 2020, 63(3): 710-719.

[20] GJB 8848-2016. Electromagnetic environmental effects test methods for system[s].